symmetry

MDPI

Article

Sensitivity Analysis of Rigid Pavement Design Based on Semi-Empirical Methods: Romanian Case Study

Costel Pleșcan [1], Elena-Loredana Pleșcan [1,*], Mariana D. Stanciu [2], Marius Botiș [1] and Daniel Taus [1]

[1] Department of Civil Engineering, Transilvania University of Brasov, Eroilor 29, 500036 Brasov, Romania; plescan.costel@unitbv.ro (C.P.); mbotis@unitbv.ro (M.B.); daniel.taus@unitbv.ro (D.T.)
[2] Department of Mechanical Engineering, Transilvania University of Brasov, Eroilor 29, 500036 Brasov, Romania; mariana.stanciu@unitbv.ro
* Correspondence: elena.puslau@student.unitbv.ro

Abstract: Due to the intensive process of road construction or rehabilitation of pavement caused by an increase in traffic volume, in the field of rigid pavement design and research in Romania, we can say that there is a need to improve the design method. In the last decade, more and more researchers have been concerned about climate change and the increase in traffic volume; hence, there is a need for a renewal of the climatological, as well as traffic, databases because these are part of the input data for the design process. The design method currently used in Romania for jointed plain concrete pavement design is NP081/2002. The limitation of the data and the lack of lifetime estimation of structural and functional performance are the main aspects that need to be addressed in the new design procedure. The Mechanistic–Empirical Pavement Design (MEPDG) method offers the possibility of the design of pavement structures by estimating the structural and functional performances. This paper aims to obtain a comparative study of these two methods for the analysis of the input data collected from the field corresponding to the three failure criteria, while the symmetry of the characteristics of the material and their asymmetrical thicknesses are compared, thus contributing to the design of viable and long-lasting pavement structures using a rigid pavement with the specific characteristics of the mountainous area in northeastern Romania on the national road DN17 Suceava—Vatra Dornei. The novelty of this study consists of the implementation of the mechanistic–empirical method MEPDG instead of the old NP081/2002 method used in Romania.

Keywords: rigid pavements; materials symmetry; thickness asymmetry; pavement design; mechanistic–empirical approach

Citation: Pleșcan, C.; Pleșcan, E.-L.; Stanciu, M.D.; Botiș, M.; Taus, D. Sensitivity Analysis of Rigid Pavement Design Based on Semi-Empirical Methods: Romanian Case Study. *Symmetry* **2021**, *13*, 168. https://doi.org/10.3390/sym13020168

Academic Editor: Raúl Baños Navarro
Received: 21 December 2020
Accepted: 18 January 2021
Published: 22 January 2021

1. Introduction

The design of road structures involves the estimation of structural and functional performances. With greater design accuracy, all maintenance and repair costs are reduced, and the corrective activities can be planned in advance. For the design of rigid pavements, over time, several methods have been developed, including predominantly theoretical (the Westergaard, Westergaard/Ioannides—USA diagram method and the Picket and Ray USA—method based on the finite element calculation scheme) and semi-empirical methods that combine theoretical design relationships with experimental results (modified Westergaard method, Highway Agency—UK method, AASHTO—American Association of State Highway and Transportation Officials method for plain concrete and for continuously reinforced concrete pavement, the MEPDG method—Mechanistic–Empirical Pavement Design USA, the Romanian method NP 081/2002, etc.) [1,2]. The semi-empirical methods have the advantage of estimating the lifetime of the pavement design on the basis of performances obtained in practice, whereas the input data allow the personalization of each case according to the climatic conditions, soil condition, pavement structure, and the traffic loads, as discussed elsewhere [3–5]. Gaspar et al. [6] and Plescan [7] presented comparative studies on the application of these methods, from the geographical and topographic point of

view, and others discussed optimization methods of the pavement design by recalibrating the obtained models [8–10]. Of all the mechanistic–empirical methods, the MEPDG method is considered one of the most realistic methods, not only for the design of pavement models but also because it offers the possibility of sizing the pavement structures by modifying the parameters of the transfer function, as discussed elsewhere [11–15]. It was found that both the loads imposed on the ground and the time accelerate the structural and functional deterioration of rigid pavements, leading to its premature failure. Therefore, the sensitivity analysis of the most significant predictive factor of pavement performance analyzed in a known geoclimatic context and under certain traffic conditions represents the current challenge of the researchers in the field, as discussed by [16,17]. Thus, the quality of a jointed plain concrete pavement (JPCP) design is given by the degree of sensitivity of the results obtained by modifying the scenario or the input dataset, as discussed by Zhu et al. and Mu et al. [18,19]. Amin [4] presented comparatively different deterministic and stochastic approaches for calculating the pavement performance curves, highlighting the advantages and disadvantages of each approach. Chong et al. [20] presented a method of multi-objective optimization of rigid pavement design starting from the objective function of reducing energy consumption and greenhouse gas emissions, in correlation with the thickness of the pavement and the surface roughness. Although the design of JPCP is carried out under the conditions of known parameters (traffic volume, climatic conditions, material), it has been found that traffic volume increases in logarithmic progression, which affects the structural and functional performances of the pavement in a shorter time than predicted by the design methods. Bayrak and Hinislioğlu [21] presented a comprehensive study that combines different analysis methods to determine the optimum thickness of the layer and the quality of the materials at a low cost–efficiency ratio.

Due to the particularities of each area, namely, environmental conditions, type of traffic, or characteristics of the base layer, the design of the road structure differs. Starting from the variability in the methods for designing the road pavement, the objective of the paper consists of a critical analysis of the efficiency of the MEPDG method for designing a jointed plain concrete pavement (JPCP). In order to achieve the proposed objective, a detailed study on the principles of the design methods for rigid pavement structures currently used in the world was undertaken, finally selecting and studying this method in detail by applying it to a significant case study in Romania located in a northeastern Romania mountain area on the National Road DN17 (E 576). This road was selected to predict the jointed plain concrete pavement models and analyze them from the performance point of view, compared to the Romanian design method according to the NP081/2002 standard. The novelty of this study consists of predicting the behavior of 72 pavement structures with different physical–mechanical characteristics, according to their response over time from the point of view of cracking, faulting, and roughness (international roughness index, IRI).

2. Summary of Basic Theory

2.1. Romanian Standard NP 081/2002

2.1.1. The Design Traffic

According to Romanian Standard NP 081/2002 "Technical recommendation for the structural design of rigid road pavements" [2], the jointed plain concrete pavement is based on the following main steps: establishing the design traffic; establishing the bearing capacity of the foundation soil; conceiving the rigid pavement structure; establishing the bearing capacity at the level of the base course; determining the thickness of the surface course. Preliminary studies have been undertaken to obtain relevant data concerning the composition, intensity, and evolution of traffic, the geotechnical characteristics of the foundation soil, and the hydrologic regime on the site, provided by the Regional Roads and Bridges Directorate Iasi. The design traffic denoted Nc is expressed in millions of standard axles and is calculated with Equation (1), as a function of the average annual daily traffic

(AADT) presented in Table 1, for a perspective period of 30 years, and a coefficient for the transversal distribution c_{rt} for the lanes of 0.50.

$$N_c = 365 * 10^{-6} * p_p * c_{rt} * \sum_{k=1}^{6} MZA * p_k * f_{ek}, \quad (1)$$

where p_p is the perspective period, c_{rt} is the transversal distribution, MZA/AADT is the annual average daily traffic, p_k is the coefficient of evolution, and f_{ek} is the equivalence coefficient.

Table 1. The variables used for design traffic calculation. AADT, average annual daily traffic.

k	Vehicle Type	AADT (Millions of Standard Axles) MZA	Coefficient of Evolution (Growth Factor) p_k	Equivalence Coefficient (ESAL-Equivalent Single Axle Load Factor) f_{ek}	$MZA*p_k*f_{ek}$
1	2 axle trucks	358	2.68	0.30	288
2	3 and 4 axle trucks	224	1.83	3.80	1558
3	Articulated vehicle	296	1.74	2.90	1494
4	Buses	81	2.30	1.50	279
5	Farm tractors	11	2.04	0.20	4
6	Road trains	46	1.48	1.60	109

Substituting the values in mathematical Equation (1) allows obtaining the design traffic Nc = 20.43 m.s.a. (millions of single axles).

2.1.2. The Bearing Capacity of the Foundation Soil

The coefficient of subgrade reaction, K_0, is determined in correlation with the climate and hydrologic regime and soil type, as given in Table 2. According to Romanian standard STAS 1709/2 [22], the hydrological regime is distributed as follows: hydrological regime 1, corresponding to the favorable conditions; hydrological regime 2, corresponding to the medium and unfavorable hydrological conditions, where 2a represents embankment road sectors, with a minimum height of 1.00 m, 2b is considered for sectors of road located in the mound with a height beneath 1.00 m, at ground height, at a mixed profile, and in cutting. Table 2 presents the soil type according to Romanian standard STAS 1243–1988 [23]. Because the road segment to which we applied the Romanian dimensioning method is characterized by soil type P3, climate type III, and hydrologic regime 2b, following Table 2, the coefficient of subgrade reaction is K_0 = 42 MN/m^3.

Table 2. Coefficient of subgrade reaction values, K_0 [23].

Climate Type	Hydrologic Regime	Soil Type				
		P_1	P_2	P_3	P_4	P_5
I	1	56	53	46	50	50
	2a	56	53	44	50	48
	2b	56	53	44	46	46
II	1	56	53	44	50	50
	2a	56	53	44	50	46
	2b	56	50	44	46	46
III	1	56	53	42	39	50
	2a	56	50	42	37	44
	2b	56	50	42	37	44

2.1.3. The Bearing Capacity at the Level of the Base Course

The bearing capacity at the level of the base course is expressed by the coefficient of reaction at the surface of the base course, K, as given in Figure 1a, which is determined as a function of the coefficient of subgrade reaction K_0 and the equivalent thickness of the base/subbase courses in cm, H_{ech}. The equivalent thickness of the base/subbase courses is calculated as the sum of the equivalent thicknesses of these layers, as given by Equation (2).

$$H_{ech} = \sum_{i=1}^{n} h_i * a_i, \quad (2)$$

where n is the number of layers, h_i is the actual thickness of the layer "i", in cm, and a_i is the equivalence coefficient for the layer "i". Knowing that the equivalence coefficient for ballast subbase is 0.75 (NP081/2002), it turns out that H_{ech} = 25 × 0.75 = 18.75 cm.

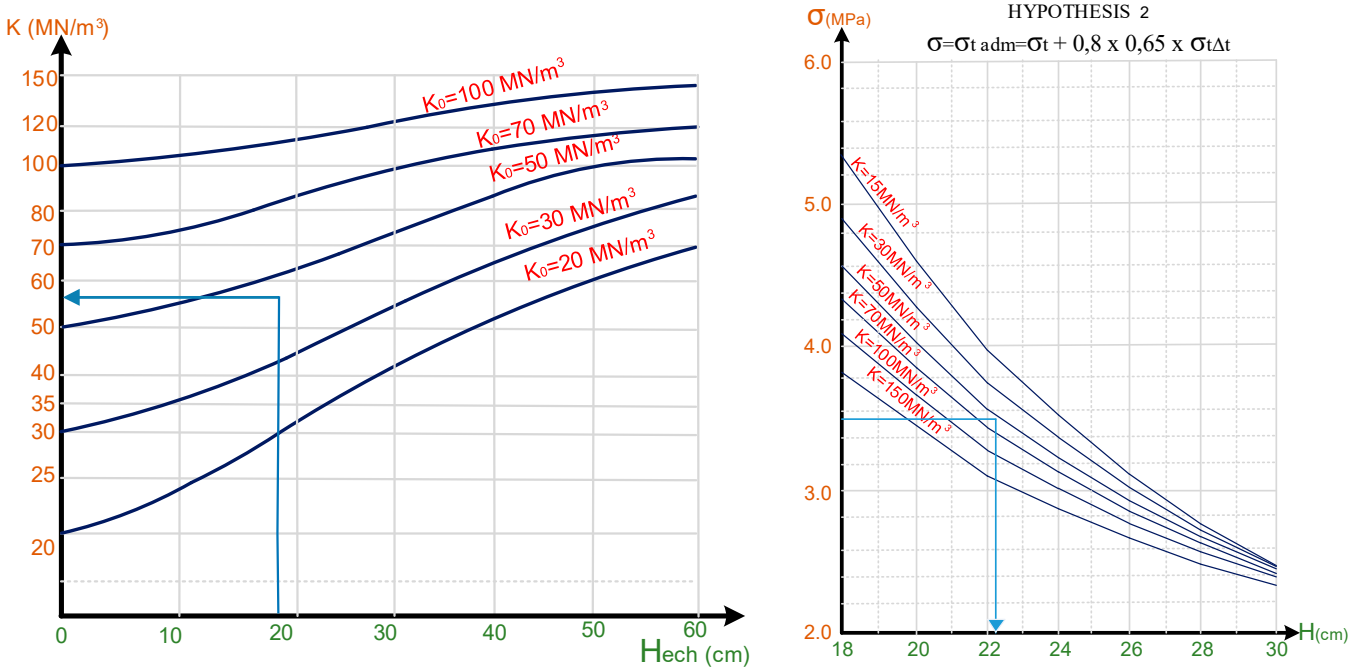

Figure 1. Design charts for determining (**a**) the bearing capacity at the level of the base course K, and (**b**) the thickness of the concrete slab H [2].

For the type of soil P3, climate type III, and hydrologic regime 2b, the dynamic elastic modulus is K = 58 MN/m^3.

2.1.4. Determining the Thickness of the Concrete Slab

The design criterion is expressed as follows (Equation (3)):

$$\sigma \leq \sigma_{t,a}, \quad (3)$$

where σ is the tensile stress from bending in the concrete slab, determined following the design hypothesis, and $\sigma_{a,t}$ is the allowable tensile stress from bending.

The allowable tensile stress from bending ($\sigma_{a,t}$) is determined using Equation (4).

$$\sigma_{a,t} = R_{inc}^{k} * \alpha * (0.70 - \gamma * logN_c), \quad (4)$$

where R_{inc}^{k} is the specific bending strength of the concrete at 28 days, α is the coefficient of concrete strength increase from 28–90 days, equal to 1.1, N_c is the traffic for the design period, and γ is a coefficient equal to 0.05.

The design hypotheses are as follows:

$\Sigma = \sigma_t + 0.8 \times \sigma_{t\Delta t} \leq \sigma\, \sigma_{t,a}$ for technical class I and II roads;

$\sigma = \sigma_t + 0.8 \times 0.65 \times \sigma_{t\Delta t} \leq \sigma\, \sigma_{t,a}$ for technical class III and IV roads;

$\sigma = \sigma_t \leq \sigma_{t,a}$, for technical class V roads.

Because the analyzed road sector has a technical class III, we chose the second hypothesis. Depending on the modulus of subgrade reaction K = 58 MN/m^3 and on the allowable flexural strength $\sigma_{t,a}$ = 3.48 MPa, the slab thickness results as $\mathbf{H_{slab}}$ **= 23 cm**, following the design diagram presented in Figure 1b.

2.2. The Mechanistic–Empirical Method MEPDG

The MEPDG method for JPCP design is illustrated by the flowchart presented in Figure 2 [24]. According to this flowchart, in the first stage, a JPCP structure is proposed that takes into consideration the specific site conditions of traffic, climatic conditions, and soil type. Then, the failure criteria are set on the basis of the desired performance that will be achieved at the end of the design life (for example, an acceptable level of faulting, cracking, and IRI for JPCP). Reliability levels are also selected for each of these performance indicators. Then, these input data are processed by the program using the finite element method for each axle type and the load over the design life. The key distresses, faulting, cracking, and roughness, are predicted month by month during the design period, using mechanistic–empirical performance models existing in the MEPDG methodology [25–27]. The roughness is then estimated on the basis of the value of the initial IRI, the distresses that occur over time, and the site conditions. The estimated performance of this structure is evaluated at the established reliability level. If the designed JPCP structure does not meet the set criteria, then it must be modified accordingly, and the design procedure applied to this modified structure is repeated.

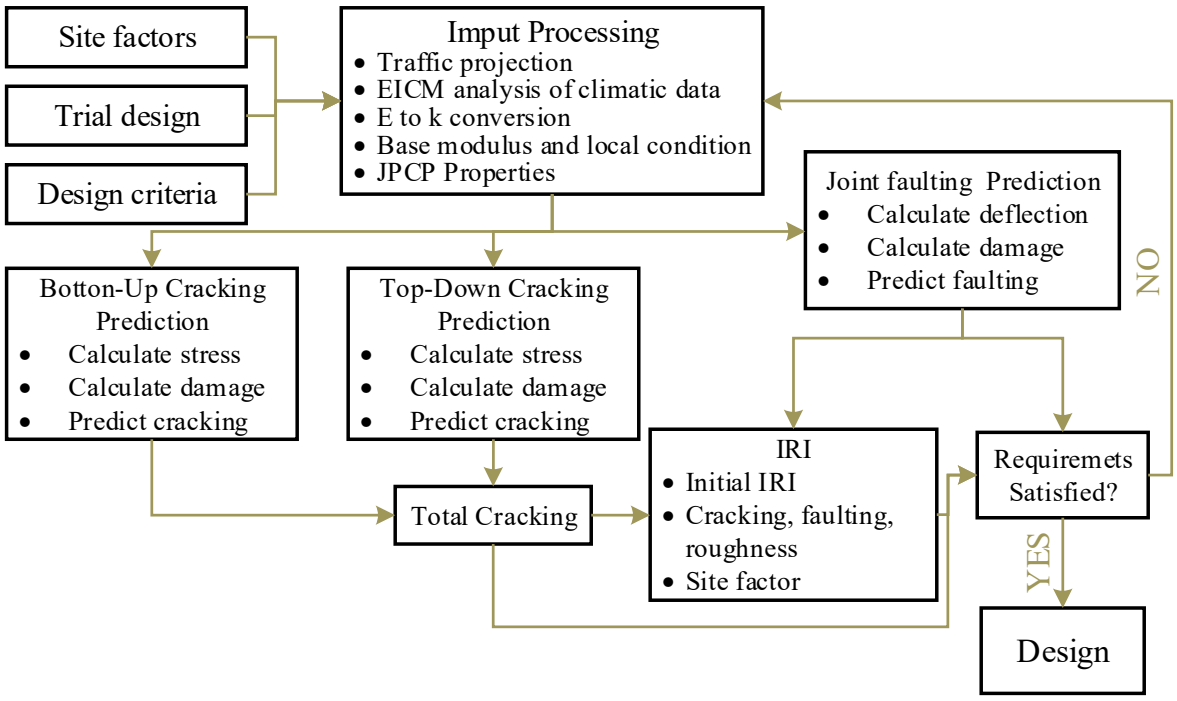

Figure 2. Flowchart for the design of jointed plain concrete pavement (JPCP) using the Mechanistic–Empirical Pavement Design (MEPDG) method [24].

3. Data Preparation Models with MEPDG Method

3.1. Climate Data for JPCP Model Development

The Romanian National Road DN17 (E 576) placed between Suceava town and Vatra Dornei city, i.e., the road sector from km 217 to 218 (Figure 3), was selected to predict the jointed plain concrete pavement models and analyzing them from the performance point of view.

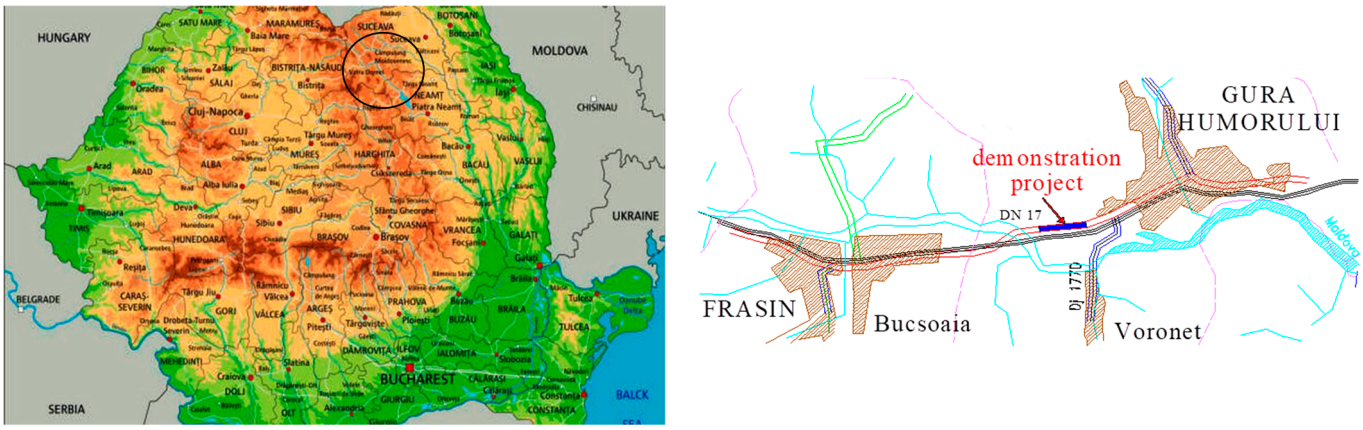

(**a**) (**b**)

Figure 3. Location of the road sector of National Road DN17: (**a**) position on Romania map; (**b**) location of road sector for analysis [7].

From the geological point of view, in this area, cohesive soils (such as silty and sandy clays) and the local slopes consist of the base layer, as considered from other sedimentary and metamorphic rocks. The climatic conditions in the area include severe winters (−250 °C) and hot summers (+30 °C) and a high level of seasonal precipitation between 1200 mm/m^2 and 1400 mm/m^2, with depth of frost between 100 and 110 cm. The data were collected from the Meteorology National Agency of Romania (ANM), Călimănești climate station. Knowing that the demonstrative road sector is located at 45.38° latitude, −89.28° longitude, 485.5 m (1593 ft) elevation, and 3 m (10 ft) depth of water table, the climate data type NARR– North American Regional Reanalysis from MEPDG software was correlated with climate data from the field.

3.2. Physical and Mechanical Characteristics of JPCP Models

According to the Romanian standard recommendation, the minimum thickness for the JPCP is 18 cm and the maximum value is 28 cm, whereas 23 cm is the thickness resulting for the case we studied with the Romanian standard NP 081/2002. For MEPDG analysis, three types of jointed plain concrete pavement models were analyzed from a thickness point of view with three asymmetric structures: 18 cm (denoted A); 23 cm (denoted B); 28 cm (denoted C) (Figure 3). In the other layers (layers 2 and 3), the geometric and structural characteristics were symmetric. Thus, the second layer was considered with the same thickness (30 mm) for all three cases and contained river-run gravel or cement-stabilized well-graded gravel. All studied variants of plain concrete pavements were analyzed assuming they have no dowels. The third layer was represented by foundation ground with infinite thickness. The length variations of rigid pavement slabs were presented in three cases: 4 m, 6 m, and 8 m. Figure 4 presents the basic matrix of JPCP.

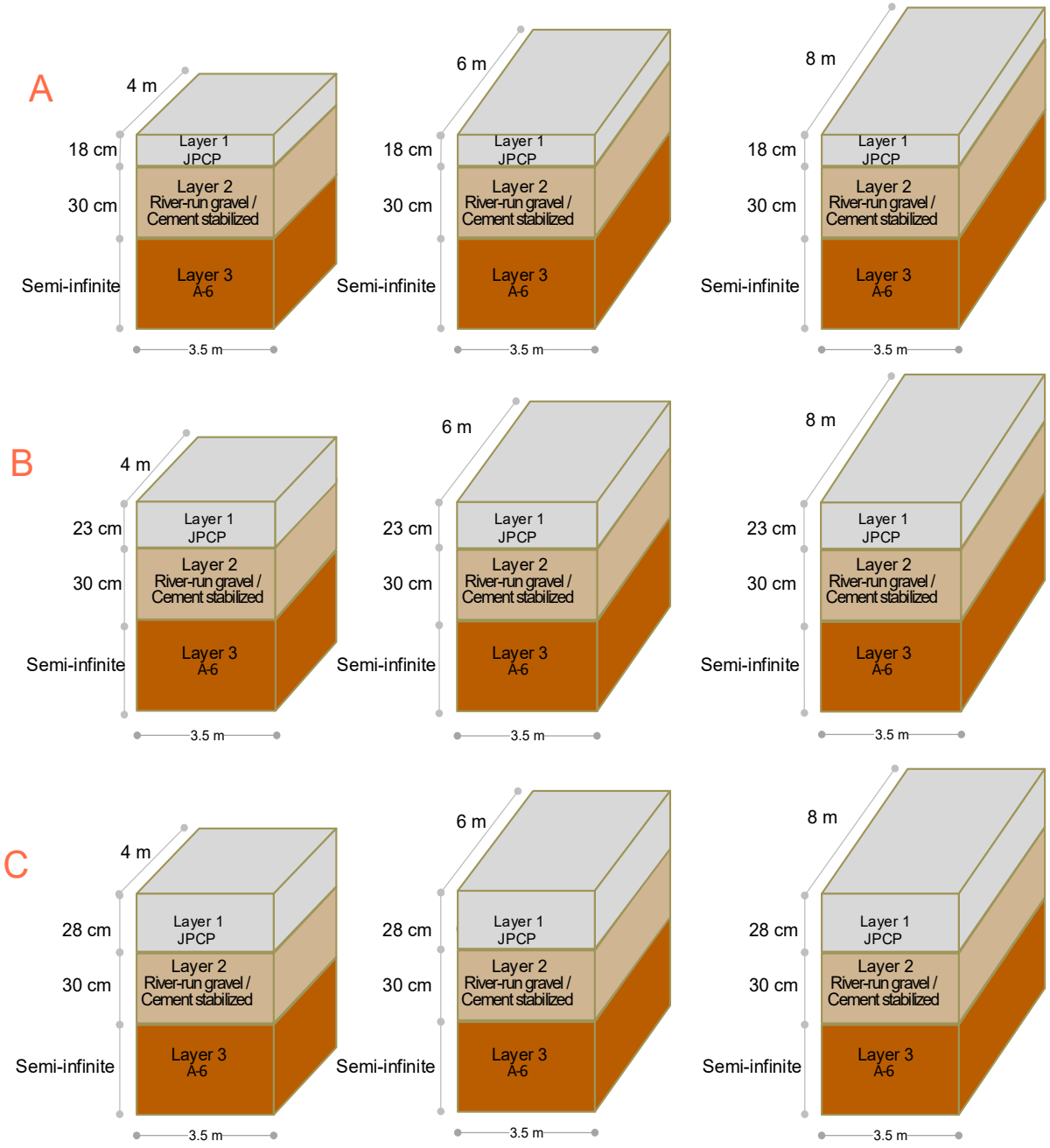

Figure 4. Types of pavement analyzed.

Applying the MEPDG method, different variables such as the thickness of the concrete slab, type of the base layer, coefficient of thermal expansion, compressive strength, and the distance between the transverse joints were applied to the simulation of JPCP lifetime behavior. Thus, the AADTT type traffic value was 1776, and the simulation was conducted by varying the mechanical characteristics of jointed plain concrete pavement: two different values of the coefficient of thermal expansion (CTE), $10 \times 10^{-6}/°C$ and $13 \times 10^{-6}/°C$; two different values of compressive strength Rc (28 days), 20 MPa and 55 MPa; unit weight, 2403 kg/m^3; 0.15 Poisson's ratio; cement type I; water/cement ratio of 0.45. Regarding the base foundation, the thickness was established at 30 cm, 0.27 Poisson's ratio, and two types of material were taken into account: river-run gravel and stabilized cement.

Combining these parameters into the MEPDG program, a total of 72 results were obtained, which allowed analysis of the variation of JPCP performance for 5, 10, 15, 20, 25, 30, and 35 years in correlation with the influence of each of the selected input parameters.

The models obtained using the MEPDG method were evaluated in terms of their behavior in cases of cracking, faulting, and roughness (IRI). The codification of each type of jointed plain concrete pavement resulting from the combination of parameters is presented in Table 3.

Table 3. The codification of studied pavement structures.

Concrete Slab Thickness (cm)	Subbase Type	Coefficient of Thermal Expansion (10^{-6}/°C)	28 Day PCC Pavement Concrete Compressive Strength (MPa)	Joint Design 4 m Code 1	Joint Design 6 m Code 2	Joint Design 8 m Code 3
18 Code **A**	River-run gravel Code **G**	10 Code **1**	20 Code **a**	AG1a1	AG1a2	AG1a3
			55 Code **b**	AG1b1	AG1b2	AG1b3
		13 Code **2**	20 Code **a**	AG2a1	AG2a2	AG2a3
			55 Code **b**	AG2b1	AG2b2	AG2b3
	Cement Stabilized Code **S**	10 Code 1	20 Code **a**	AS1a1	AS1a2	AS1a3
			55 Code **b**	AS1b1	AS1b2	AS1b3
		13 Code **2**	20 Code **a**	AS2a1	AS2a2	AS2a3
			55 Code **b**	AS2b1	AS2b2	AS2b3
23 Code **B**	River-run gravel Code **G**	10 Code **1**	20 Code **a**	BG1a1	BG1a2	BG1a3
			55 Code **b**	BG1b1	BG1b2	BG1b3
		13 Code **2**	20 Code **a**	BG2a1	BG2a2	BG2a3
			55 Code **b**	BG2b1	BG2b2	BG2b3
	Cement Stabilized Code **S**	10 Code **1**	20 Code **a**	BS1a1	BS1a2	BS1a3
			55 Code **b**	BS1b1	BS1b2	BS1b3
		13 Code **2**	20 Code **a**	BS2a1	BS2a2	BS2a3
			55 Code **b**	BS2b1	BS2b2	BS2b3
28 Code **C**	River-run gravel Code **G**	10 Code **1**	20 Code **a**	CG1a1	CG1a2	CG1a3
			55 Code **b**	CG1b1	CG1b2	CG1b3
		13 Code **2**	20 Code **a**	CG2a1	CG2a2	CG2a3
			55 Code **b**	CG2b1	CG2b2	CG2b3
	Cement Stabilized Code **S**	10 Code **1**	20 Code **a**	CS1a1	CS1a2	CS1a3
			55 Code **b**	CS1b1	CS1b2	CS1b3
		13 Code **2**	20 Code **a**	CS1a1	CS2a2	CS2a3
			55 Code **b**	CS2b1	CS2b2	CS2a3

For the presented study, the Mechanistic–Empirical Pavement Design Guide (MEPDG) developed under the National Cooperative Highway Research Program (NCHRP) Project 1–37A, version 1.003/2007 AASHTO's DARWin-ME, was used.

4. Results and Discussion

The analysis performed using the MEPDG method highlighted the response of all 72 structural variants established for the design life for the traffic loads and the predetermined climatic conditions, being useful in establishing the decisions regarding the rehabilitation of any road structure similar to that in the presented study. According to [1], the most important performance criteria for rigid pavements are cracking, faulting, and roughness of concrete slab surfaces. Thus, the obtained results are presented concerning the three performance criteria.

4.1. Estimation of Cracking

The most important degradation recorded by plain concrete pavement structures is their cracking. Thus, transverse cracks of the concrete slabs can occur at the surface of the concrete slab and propagate down (top-down cracking) or at the base of the concrete slab (bottom-up cracking) depending on the load and environmental conditions, properties of the materials, design features, and the conditions during construction. Bottom-up transverse cracking is caused by tensile bending stress at the bottom of the PCC – Pavement Concrete Compressive Strength slab, midway between two transverse joints [28,29]. Repeated heavy axle loading and a high positive temperature gradient (the top of the slab is warmer than the bottom of the slab) cause fatigue damage to occur along the bottom of the slab. This fatigue damage results in a transverse crack of the pavement that can propagate to the surface. Bottom-up transverse cracking is combined with top-down transverse cracking and calculated as a percentage of slabs cracked [30,31]. Transverse cracks of JPCP may have a small impact on overall structure performance as long as they have not evolved too much. Structural performance is influenced by transverse cracks when dynamic loads from the rigid pavements with a high roughness reduce the pavement life [18]. Transverse cracks can be caused by the uneven distribution of loads to the joints of the irregularity of the surface of the subbase, the insufficient thickness of the slab, and the shortcomings of the quality of the materials used. The influence of each parameter on the cracking of the concrete slab is presented below. Figure 5 presents the variation of cracking during the design life. With the increasing distance of the joints (length of the slab), an increase in cracking percentage of the slab of about 53.5% can be observed (Figure 5). The increase in compressive strength of concrete from 20 MPa to 55 MPa led to a decrease in the cracking percentage of the concrete slab to 1.1% (length of 4 m). Increasing the distance between the joints (6 m, 8 m) led to a decrease in cracking resistance.

Thus, it can be considered that the structure AG1b1, with a granular base layer, showed the best behavior between the concrete strength and the distance between the joints. From the point of view of the JPCP with a stabilized base layer, a similar behavior to that of a granular base layer can be noted, with the rate of occurrence of cracks reduced. Thus, in the case of the granular base layer with a concrete slab with a length of 8 m and a compressive strength of 20 MPa (structure AG1a3), it predicts the occurrence of 40% of cracks in 2.5 years. In the case of a stabilized ballast structure, the cracking percentage of 40% occurs after approximately 15 years for the AS1a3 structure (Figure 5). From the point of view of structural resistance to cracks, two optimal pavement types can be considered: AS1b1 and AS1b2. Figure 6 presents the sensitivity analysis of cracked concrete slabs with the smallest variation of percentage cracking in time.

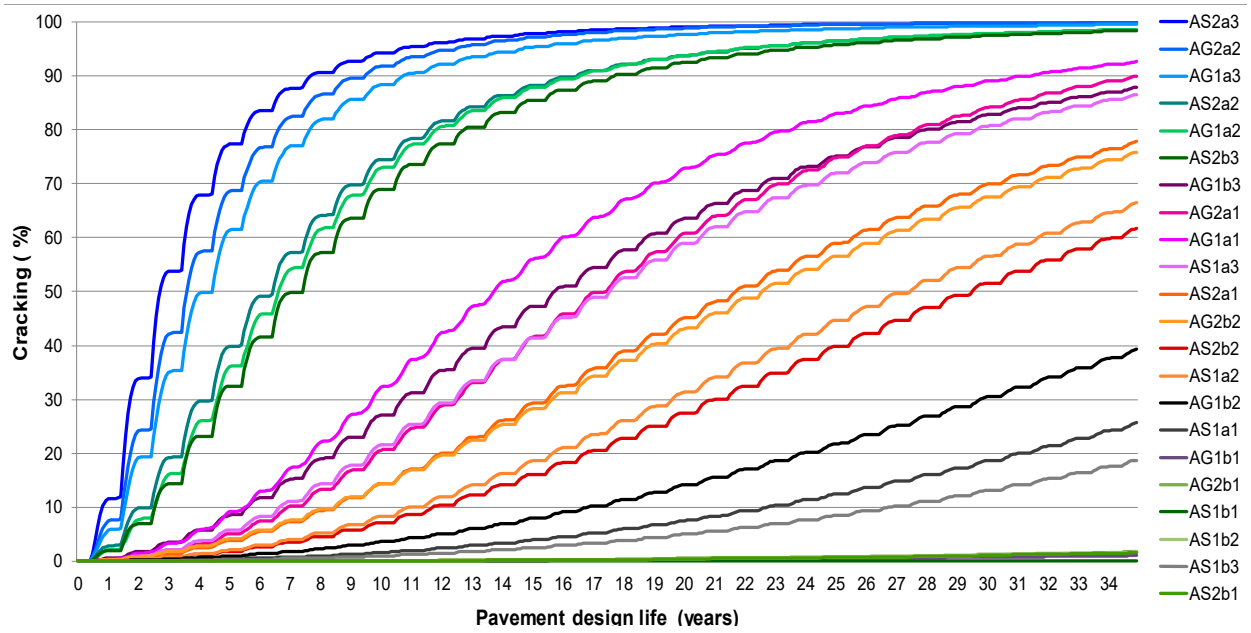

Figure 5. Lifetime prediction of cracking for different JPCPs.

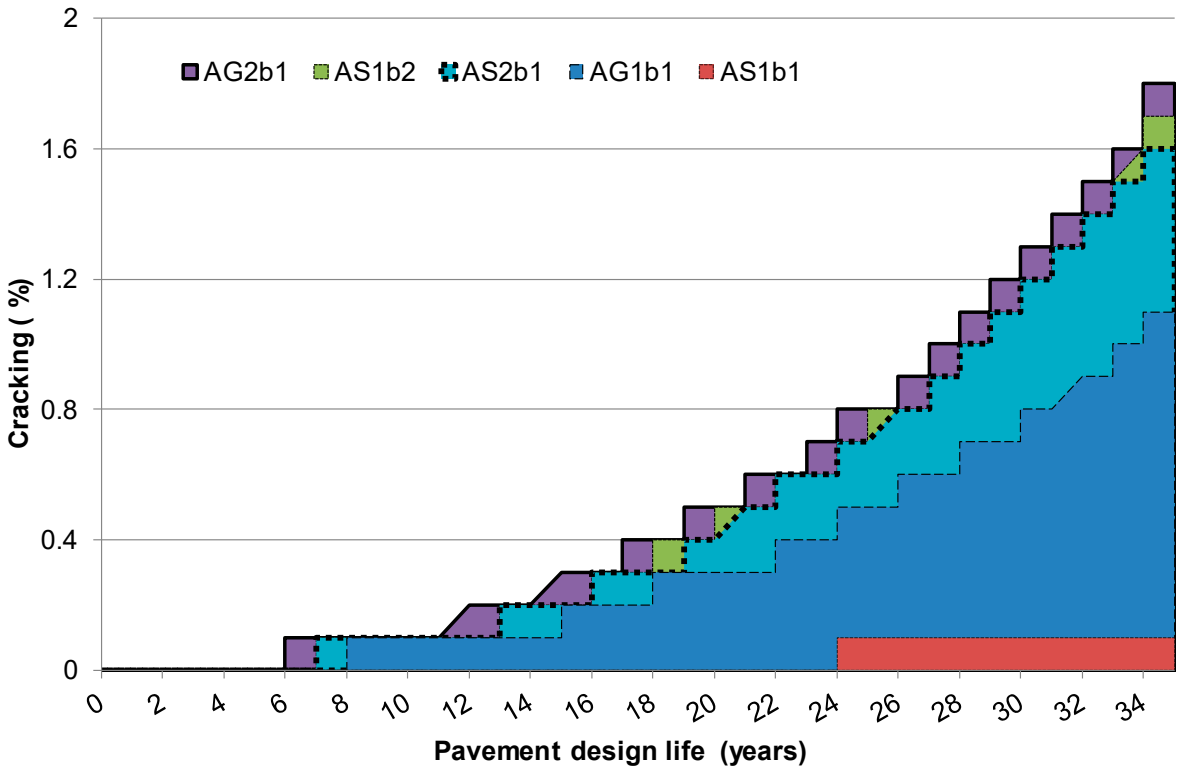

Figure 6. Sensitivity analysis of cracking propagation in the case of JPCP with the smallest variation of cracking percentage in time.

It can be seen that the AS1b1 structure showed the lowest values of the cracking percentage, which is characterized by a stabilized base layer, a concrete slab with a length of 4 m, CTE = 10, and a compressive strength of 55 MPa concrete. From the efficiency point of view, all the variants determined using the MEPDG method in Figure 6 can be taken into consideration in the design calculation, as the values of the cracking percentage were

recorded below 5% during the 35 years. Cracks occurred due to repeated loading, leading to compressive stress. Once the cracks appeared, they propagated from the bottom up. An important factor that led to the increase in cracking rate on the Romanian traffic section was the variation in extreme temperatures during the year, which led to the expansion phenomenon and contraction of the water accumulated in the concrete pores or the interfaces between the JPCP layers. The MEPDG crack analysis resulted in a matrix of the rigid pavement with the lowest percentage of cracking, up to a maximum percentage of 50% over 35 years of the pavement life, as can be seen in Table 4.

Table 4. Sensitivity matrix of pavement relative to the percentage of cracking.

0%	<1%	1–10%	10–50%
BG1b1	AS1b1	AG1b1	AG1b2
BG1b2	BG1a1	AG2b1	AS1a1
BG2b1	BG2b2	AS1b2	AS1b3
BS1b1	BS1a1	AS2b1	BG1a2
BS1b2	BS2b2	BG2a1	BG1b3
BS2b1	CG1a2	BS1b3	BS1a2
CG1a1	CG1b3	BS2a1	CG2b3
CG1b1	CG2a1	CG2a2	CS1a3
CG1b2	CS1a2	CS2a2	
CG2b1	CS2a1		
CG2b2			
CS1b1			
CS1b2			
CS1b3			
CS2b1			
CS2b2			

4.2. Estimation of Faulting

The level difference between the edges of two adjacent slabs, at a transverse or longitudinal joint, represents another criterion for evaluating the performance of a JPCP, known as faulting. This distress can be caused by repeated heavy axle loads, poor joint load transfer efficiency, free moisture below the concrete slab, erosion of the base, subbase, subgrade, or shoulder material, and upward curling of the slab [32]. Transverse joint faulting is a measurement of the differential deflection across a joint, and the admissible value is 0.19685 inches (5 mm). The modeling results revealed that the lowest average faulting values were obtained for the 28 cm thick slab, reaching the admissible value in about 30 years. In the case of the 18 cm thick slab, faulting occurred after approximately 15 years, and, in the case of 23 cm thick slab, faulting occurred after 25 years (see Figure 7).

The stabilized base is a cemented, rigid material that distributes the load over a large area, and stresses in the subgrade are reduced, which provides excellent support for the concrete slab of a rigid pavement. The stabilized base material is stronger, uniform, and more water-resistant than a granular base. The use of cement-stabilized bases reduces the occurrence of faulting, as can be seen in Figure 8. Thus, the different behavior of the base layer is manifested by a decrease of approximately 85% in the case of the stabilized ballast layer compared to the granular layer after 5 years. Increasing the strength of concrete from 20 MPa to 50 MPa contributes to increasing the rigidity of the road structure to about 50% after 5–10 years.

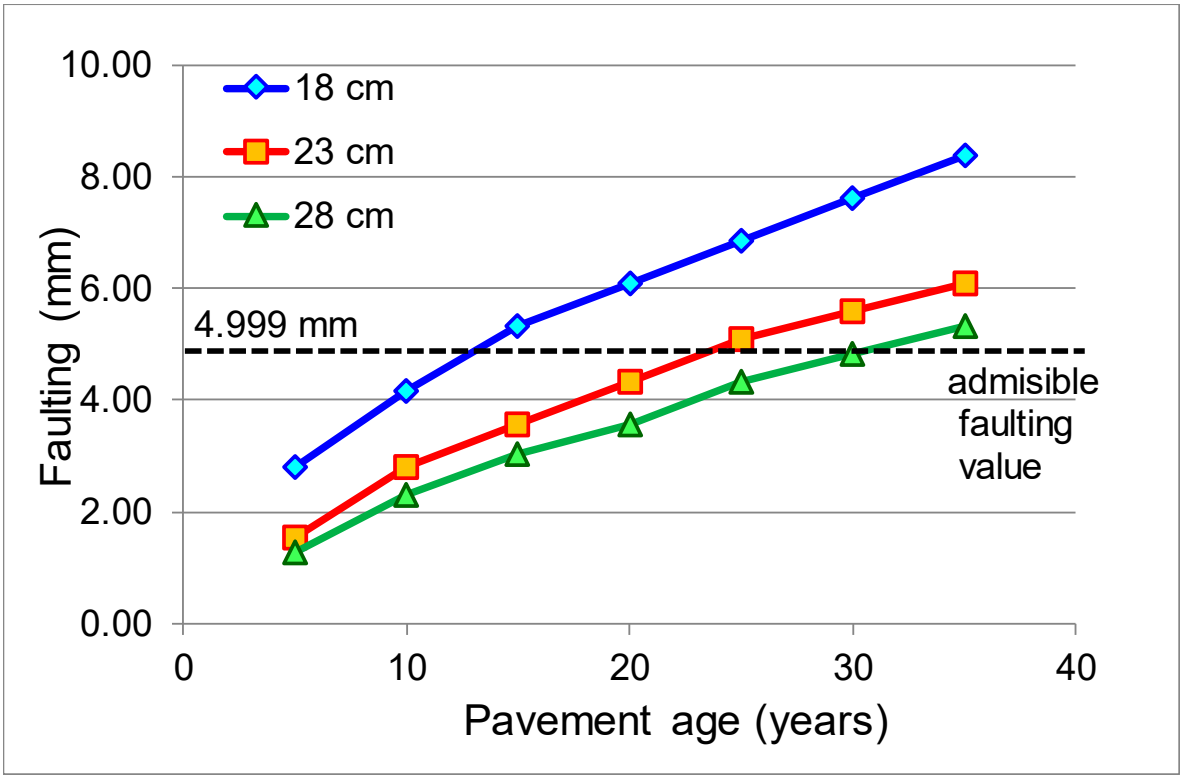

Figure 7. Variation in time of faulting depending on the thickness of concrete slabs.

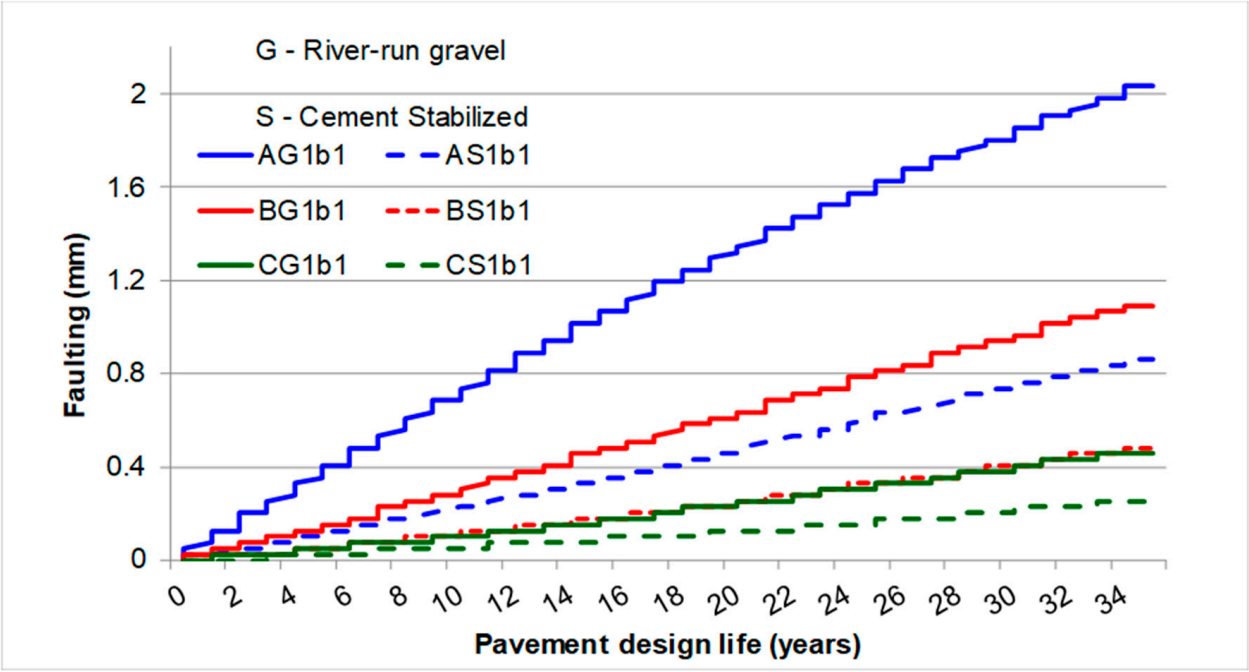

Figure 8. Lifetime prediction of faulting for different types of JPCPs.

Table 5 presents the influences of each parameter taken into account related to the admissible value of faulting (0.196585 in, 0.5 cm). Thus, it can be noticed that the values lower than 100% fall within the admissible values, while the highest are variants of road structures that no longer meet this criterion at any given time. Therefore, in terms of the thickness of the concrete slabs (coded A, B, C), the tiles with the largest thickness (28 cm) recorded the lowest values of the faulting. The stabilized ballast provided a better pavement structure behavior, and the coefficient of expansion CTE = 13 × 10^{-6}/°C favored the occurrence of faulting with values about 66% higher than CTE = 10 × 10^{-6}/°C. Doubling the distance between the joints and the length of the concrete slab increased the compaction by approximately 50% in the first 5 years. Starting with the 15th year of pavement life, the structures with a small thickness of the slab and highest length with river-run gravel subbase and a high coefficient expansion would require maintenance work. The results of MEPDG analysis highlighted that from 72 variants of JPCPs, 64 hypothetical cases met the condition whereby faulting was less than the nominal value (0.19685 in, 0.5 cm).

Table 5. Percentage values related to admissible values of faulting.

Input Data		Faulting Related to Admissible Value (%)						
		5	**10**	**15**	**20**	**25**	**30**	**35**
Slab thickness (cm)	A	55.880	86.360	106.680	121.920	137.160	152.400	167.640
	B	30.480	55.880	71.120	86.360	101.600	111.760	121.920
	C	25.400	45.720	60.960	71.120	86.360	96.520	106.680
Subbase (cm)	G	55.880	86.360	111.760	127.000	142.240	157.480	172.720
	S	20.320	35.560	50.800	60.960	71.120	81.280	91.440
CTE (10^{-6}/°C)	10	15.240	30.480	40.640	55.880	66.040	71.120	81.280
	13	60.960	91.440	116.840	137.160	152.400	167.640	177.800
Rc (28 days) (MPa)	20	30.480	50.800	71.120	86.360	96.520	106.680	121.920
	55	45.720	71.120	91.440	106.680	116.840	132.080	142.240
Distance between joints (m)	4	15.240	30.480	45.720	55.880	66.040	76.200	86.360
	6	30.480	50.800	66.040	81.280	96.520	106.680	116.840
	8	66.040	101.600	127.000	147.320	162.560	172.720	187.960

4.3. Evaluation of International Roughness Index (IRI)

Pavement roughness is used as a composite index of pavement quality and is directly related to overall ride quality, the factor of most importance to highway users. Because of these reasons, empirical roughness prediction models have been incorporated in the MEPDG, being characterized in terms of the IRI, measured in inches of roughness per miles in American standard (measured in meters/kilometers in Romanian Standard NP 081/2002). IRI depends on the initial input parameters used for pavement design and the climatic conditions that may affect roughness of the road through mechanisms such as shrinkage or swelling of subgrade soils and frost. IRI was established by Sayers et al. in 1986 as an internationally accepted parameter, and it is determined with specialized vehicles that measured the displacement of the vehicle chassis placed on the rear axle [32,33]. The IRI threshold recommended by the FHWA (Federal Highway Administration of USA) in 1998 is 95–170 in/mi for acceptable ride quality and less than 95 in/mi for good road quality, being considered the most international index for pavement roughness measurement [3]. In 2008, DDOT (District Department of Transportation, USA) changed the IRI threshold in PCI (pavement condition index) for bituminous and concrete pavement in cases of urban road, as summarized by Arhin et al. [34] and Perez et al. [35]. Table 6 presents the IRI values relative to lifetime prediction. Analyzing the influence of the various parameters on the cumulative IRI values for 35 years, it is noted that, for an 18 cm thick concrete slab, a deviation from smoothness is recorded after 20 years, and a 38% increase in the thickness of the concrete slab leads to a 25% increase in the service life, which is within acceptable limits (see Table 6). The use of a stabilized cement base layer leads to a 75% increase in the

operating life below 170 inches per mile compared to the duration of the granular subbase. The same aspect is also noticeable when a lower thermal expansion coefficient is used, being reduced by approximately 23% (e.g., CTE 10 (10^{-6}/°C)). The use of a low-strength concrete (20 MPa) leads to the appearance of surface roughness exceeding acceptable limits after 23 years of service life, and doubling the distance between the joints would lead to the appearance of roughness over acceptable limits in only 20 years (Table 6). From the MEPDG simulation, it was observed that none of the road structures showed values below 95 in/mile, but there was a set of variants with an IRI index below 170 in/mi, as can be seen in Table 7.

Table 6. Lifetime prediction of international roughness index (IRI) values.

Input Data		IRI m/km						
		5	10	15	20	25	30	35
Pavement thickness (cm)	18	1.66	2.13	2.50	2.84	3.29	3.55	3.78
	23	1.40	1.75	2.02	2.37	2.66	2.89	3.11
	28	1.35	1.57	1.81	2.04	2.30	2.51	2.70
Sub base (cm)	River-run gravel	1.58	2.00	2.32	2.65	3.03	3.27	3.50
	Cement stabilized	1.36	1.63	1.90	2.19	2.47	2.69	2.90
CTE (10^{-6}/°C)	CTE 10	1.27	1.56	1.83	2.10	2.38	2.60	2.80
	CTE 13	1.69	2.11	2.43	2.77	3.17	3.41	3.64
Rc (28 days), MPa	Rc 20 MPa	1.55	1.95	2.26	2.62	2.97	3.21	3.43
	Rc 55 MPa	1.39	1.69	1.96	2.21	2.53	2.75	2.97
Distance between joints (m)	4 m	1.28	1.57	1.86	2.15	2.44	2.67	2.89
	6 m	1.35	1.69	1.94	2.28	2.68	2.92	3.13
	8 m	1.78	2.18	2.46	2.75	3.04	3.27	3.48

Table 7. Sensitivity matrix of pavement related to IRI.

95–170 in/miles (1.4994–2.683 m/km)		
AS1b1	AS1b2	AS1b3
BG1b1	BG1b2	BS1b3
BS1a1	BS1a2	CG1b3
BS1b1	BS1b2	CS1b3
BS2b1	CG1a2	
CG1a1	CG1b2	
CG1b1	CG2b2	
CS1a1	CS1a2	
CS1b1	CS1b2	
CS2b1	CS2b2	
	CG2b2	

5. Conclusions

The paper presented the lifetime prediction of jointed plain concrete pavement for a real traffic road segment analyzed using two methods: one according to Romanian standards and the other according to the more comprehensive MEPDG method. The estimation of the dimensions (thickness) of jointed plain concrete pavement using the Romanian Standard NP 081/2002 was very close to the MEPDG method (23 cm) but poorer and without time estimation of structural and functional performance. The MEPDG method analyzed the influence of each parameter, offering a realistic analysis as a function of the cumulative effect of these factors, such that the solutions obtained by the sensitivity method returned only the variants of the road structure that simultaneously fulfilled the three requirements of structural and functional performance—cracking, faulting, and IRI. Table 8 presents the seven solutions out of the 72 analyzed which can be chosen for the

design of the pavement structures in traffic conditions and an environment specific to a temperate mountainous region, with temperature variations and annual humidity specific to the northern Romania area.

Table 8. The optimal variants of road structure that comply simultaneously with the three criteria of structural and functional performance.

Variants	Percentage of Slabs Cracked (<1%)	Faulting (<0.03937 in) (1 mm)	IRI (95–170 in/miles) (1.4994–2.683 m/km))
1	AS1b1	AS1b1	AS1b1
2	BS1b1	BS1b1	BS1b1
3	CG1a1	CG1a1	CG1a1
4	CG1b1	CG1b1	CG1b1
5	CS1b1	CS1b1	CS1b1
6	CS1b2	CS1b2	CS1b2
7	CS1b3	CS1b3	CS1b3

In conclusion, the analyses performed in this significant study highlight the critical design phases within the MEPDG methodology, as well as possibilities for applying this method in other countries where national standards are based on classical methods. From a practical point of view, the presented study highlights how the MEPDG method can objectively lead to the elimination of possible variants of JPCP that do not simultaneously meet the requirements of structural and functional performance. From the results, the constructor or the beneficiary can choose the most convenient variant from the financial point of view.

Author Contributions: Conceptualization, C.P. and E.-L.P.; methodology, C.P.; software, E.-L.P.; validation, C.P., E.-L.P., M.D.S., M.B. and D.T.; formal analysis, M.D.S., M.B. and D.T.; investigation, E.-L.P.; resources, M.D.S., M.B. and D.T.; data curation, C.P. and E.-L.P.; writing—original draft preparation, C.P.; writing—review and editing, E.-L.P.; visualization, M.B.; supervision, M.D.S. and M.B.; project administration, E.-L.P.; funding acquisition, M.D.S. All authors have read and agreed to the published version of the manuscript.

Funding: This study was conducted within the Doctoral Program BRAIN, POSDRU/6/1.5/S/9 [No.6681].

Institutional Review Board Statement: Not applicable.

Informed Consent Statement: Not applicable.

Data Availability Statement: Not applicable.

Acknowledgments: The authors are thankful to Radu Andrei and Boboc Vasile from Cheorghe Asachi Technical University of Iasi for administrative and technical support.

Conflicts of Interest: The authors declare no conflict of interest.

References

1. NCHRP. Guide for mechanistic–empirical design of new and rehabilitated pavement structures. In Proceedings of the 2004 Annual Conference and Exhibition of the Transportation Association of Canada-Transportation Innovation-Accelerating the Pace, Quebec, QC, Canada, 19–22 September 2004.
2. *NP 081/2002 Technical Recommendation for the Structural Design of Rigid Road Pavements—Romanian Standard*; Bucharest, Roamania.
3. Prozzi, J.A.; Madanat, S.M. Development of pavement performance models by combining experimental and field data. *J. Infrastruct. Syst.* **2004**, *10*, 9–22. [CrossRef]
4. Amin, M.S.R. The pavement performance modeling: Deterministic vs. stochastic approaches. In *Numerical Methods for Reliability and Safety Assessment: Multiscale and Multiphysics Systems*, 1st ed.; Kadry, S., El Hami, A., Eds.; Springer: Cham, Switzerland, 2014. [CrossRef]

5. Timm, D.; Birgisson, B.; Newcomb, D. Development of mechanistic-empirical pavement design in Minnesota. *Transp. Res. Rec.* **1998**, *1629*, 181–188. [CrossRef]
6. Gáspár, L.; Veeraragavan, A.; Bakó, A. Comparison of road pavement performance modelling of India and Hungary. *Acta Tech. Jaurinensis* **2009**, *2*, 35–55. Available online: http://journal.sze.hu/index.php/acta/article/view/205 (accessed on 8 October 2020).
7. Plescan, E.L.; Plescan, C. Implementation of mechanistic-empirical pavement design guide ME-PDG in Romania. *BUT Braşov.* **2014**, *7*, 323–328.
8. Carvalho, R.; Ayres, M.; Shirazi, H.; Selezneva, O.; Darter, M. Impact of Design Features on Pavement Response and Performance in Rehabilitated Flexible and Rigid Pavements. FHWA. 2011. Available online: https://www.fhwa.dot.gov/publications/research/infrastructure/pavements/ltpp/10066/10066.pdf (accessed on 8 October 2020).
9. Ameri, M.; Khavandi, A. Development of mechanistic-empirical flexible pavement design in Iran. *J. Appl. Sci.* **2009**, *9*, 354–359. [CrossRef]
10. Guo, S.; Dai, Q.; Hiller, J. Investigation on the freeze-thaw damage to the jointed plain concrete pavement under different climate conditions. *Front. Struct. Civ. Eng.* **2018**, *12*, 227–238. [CrossRef]
11. Bordelon, A.C.; Roesler, J.; Hiller, J.E. *Mechanistic-Empirical Design Concepts for Jointed Plain Concrete Pavements in Illinois*; Illinois Center for Transportation (ICT): Springfield, IL, USA, 2009; Available online: http://hdl.handle.net/2142/15210 (accessed on 8 July 2020).
12. Li, Q.; Xiao, D.X.; Wang, K.C.P.; Hall, K.D.; Qiu, Y. Mechanistic-Empirical Pavement Design Guide (MEPDG): A bird's-eye view. *J. Mod. Transp.* **2011**, *19*, 114–133. [CrossRef]
13. Islam, S.; Sufian, A.; Hossain, M.; Velasquez, N.; Barrett, R. Practical issues in implementation of mechanistic empirical design for concrete pavements. *J. Transp. Eng. Part Pavements* **2019**, *145*. [CrossRef]
14. Harsini, I.; Haider, S.W.; Brink, W.C.; Buch, N.; Chatti, K. Investigation of significant inputs for pavement rehabilitation design in the pavement-me. *Can. J. Civ. Eng.* **2018**, *45*, 386–392. [CrossRef]
15. Eyada, S.O.; Celik, O.N. A plan for the implementation of mechanistic-empirical pavement design guide in Turkey. *Pertanika J. Sci. Technol.* **2018**, *26*, 1927–1949.
16. Jannat, G.; Tighe, S.L. An experimental design-based evaluation of sensitivities of MEPDG prediction: Investigating main and interaction effects. *Int. J. Pavement Eng.* **2016**, *17*, 615–625. [CrossRef]
17. Zhong, J. Rigid Pavement: Ontario Calibration of the Mechanistic-Empirical Pavement Design Guide Prediction Models. Master's Thesis, Master of Applied Science in Civil Engineering, University of Waterloo, Waterloo, ON, Canada, 2017.
18. Zhu, Y.; Ni, F.; Li, H. Calibration and sensitivity analysis of rut prediction model for semi-rigid pavement using AASHTOWare ME design. *Road Mater. Pavement Des.* **2017**, *18*, 23–32. [CrossRef]
19. Mu, F.; Vandenbossche, J.M.; Gatti, K.A.; Sherwood, J.A. An evaluation of JPCP faulting and transverse cracking models of the mechanistic-empirical pavement design guide. *Road Mater. Pavement Des.* **2012**, *13*, 128–141. [CrossRef]
20. Chong, D.; Wang, Y.; Dai, Z.; Chen, X.; Wang, D.; Oeser, M. Multiobjective optimization of asphalt pavement design and maintenance decisions based on sustainability principles and mechanistic-empirical pavement analysis. *Int. J. Sustain. Transp.* **2018**, *12*, 461–472. [CrossRef]
21. Bayrak, O.Ü.; Hınıslıoğlu, S. A new approach to the design of rigid pavement: Single-Axle loading. *Road Mater. Pavement Des.* **2017**, *18*, 573–589. [CrossRef]
22. STAS 1709/2 Road Works. *The Action of the Freeze-Thaw Phenomenon in Road Works*; Buchaarest, Romania.
23. *STAS 1243-1988 Soil Classification and Identification*; Buchaarest, Romania.
24. National Cooperative Highway Research Program Transportation Research Board (NCHRP). *Guide for Mechanistic-Empirical Design of New and Rehabilitated Pavement Structures*; Transportation Association of Canada (TAC): Ottawa, ON, Canada, 2004.
25. Ceylan, H.; Kim, S.; Gopalakrishnan, K.; Schwartz, C.W.; Li, R. Sensitivity analysis frameworks for mechanistic-empirical pavement design of continuously reinforced concrete pavements. *Constr. Build. Mater.* **2014**, *73*, 498–508. [CrossRef]
26. Hall, K.D.; Beam, S. Estimating the sensitivity of design input variables for rigid pavement analysis with a mechanistic-empirical design guide. *Transp. Res. Rec.* **2005**, *1919*, 65–73. [CrossRef]
27. Hajek, J.J.; Billing, J.R.; Swan, D.J. Forecasting traffic loads for mechanistic-empirical pavement design. *Transp. Res. Rec.* **2011**, *2256*, 151–158. [CrossRef]
28. Bhattacharya, B.B.; Gotlif, A.; Darter, M.I.; Khazanovich, L. Impact of joint spacing on bonded concrete overlay of existing asphalt pavement in the AASHTOWare pavement ME design software. *J. Transp. Eng. Part Pavements* **2019**, *145*, 1–9. [CrossRef]
29. Xu, C.; Cebon, D. *Analysis of Cracking in Jointed Plain Concrete Pavements*; Federal Highway Administration (FHWA) Georgetown: Washington, DC, USA, 2017.
30. Guclu, A.; Ceylan, H.; Gopalakrishnan, K.; Kim, S. Sensitivity Analysis of Rigid Pavement Systems Using the Mechanistic-Empirical Design Guide Software. *J. Transp. Eng.* **2009**, *135*, 555–562. [CrossRef]
31. American Association of State Highway and Transportation Officials Executive Committee. Performance Indicator Prediction Methodologies. In *Mechanistic—Empirical Design Guide, a Manual of Practice*; American Association of State Highway and Transportation Officials: Washington, DC, USA, 2008; pp. 33–49.

32. Sayers, M.W.; Gillespie, T.D.; Queiroz, C.A.V. *The International Road Roughness Experiment (IRRE): Establishing Correlation and a Calibration Standard for Measurements*; World Bank Group: Washington, DC, USA, 1986.
33. Sayers, M.W.; Gillespie, T.D.; Paterson, W.D.O. *Guidelines for Conducting and Calibrating Road Roughness Measurements*; The World Bank: Washington, DC, USA, 1986.
34. Arhin, S.A.; Noel, E.C.; Ribbiso, A. Acceptable international roughness index thresholds based on present serviceability rating. *J. Civ. Eng. Res.* **2015**, *5*, 90–96.
35. Pérez-Acebo, H.; Mindra, N.; Railean, A.; Rojí, E. Rigid pavement performance models by means of markov chains with half-year step time. *Int. J. Pavement Eng.* **2019**, *20*, 830–843. [CrossRef]